

Reduction of interfilament contact loss in Nb₃Sn superconductor wires

R. B. Goldfarb

National Institute of Standards and Technology, Boulder, Colorado 80303

K. Itoh

National Research Institute for Metals, Tsukuba, Ibaraki 305, Japan

(Received 28 September 1993; accepted for publication 2 November 1993)

Interfilament contact in Nb₃Sn wires made by the internal-tin-diffusion process causes excess hysteresis loss beyond the intrinsic magnetic hysteresis loss of the filaments. In analogy with eddy-current and proximity-effect coupling losses, the excess contact loss can be reduced by decreasing the twist-pitch length of the filaments in the wire. One consequence of interfilament contact is that volume magnetization measurements are strongly dependent on sample length below about one twist pitch. We define a characteristic length whose reciprocal is equal to the sum of the reciprocals of the sample length and the twist pitch. Hysteresis loss is a universal function of characteristic length for different sample lengths and twist pitches. We discuss several experimental parameters for the magnetic determination of hysteresis loss.

I. INTERFILAMENT COUPLING IN SUPERCONDUCTOR WIRES

Multifilamentary Nb₃Sn wires often exhibit interfilament contact and a concomitant increase in magnetic hysteresis loss above that due to the intrinsic magnetic hysteresis of the filaments. In *in situ* processed Nb₃Sn, the excess loss was attributed to intermittent filament contact by Shen^{1,2} and Braginski.^{3,4} In wires made by the internal-tin-diffusion process, it has been ascribed to bridging between filaments.⁵⁻⁷ With reference to the critical-state model for the magnetization of superconductors, the excess loss is sometimes quantified in terms of an increased effective filament diameter.

Other possible sources of interfilament coupling can give rise to excess loss: eddy-current and proximity-effect coupling. Time-dependent interfilament coupling by eddy currents in the matrix occurs when filamentary conductors are exposed to changing fields. Such eddy-current coupling may be reduced by twisting the wire and the filaments during manufacture.^{8,9} This has become standard practice in the industry, and twist-pitch lengths of 10–30 mm are typical. Volume magnetization can depend on the length of the sample, where a short sample has an effective twist pitch equal to the sample length.^{8,10} Twisting also reduces time-independent proximity effect between the filaments and its associated excess loss.¹¹⁻¹³

We find that, in internal-tin Nb₃Sn, interfilament contact actually may be continuous. The excess contact loss is time independent and occurs at all fields, including fields above which any proximity effect would be destroyed. We show that, like eddy-current and proximity-coupling losses, contact loss may be reduced by decreasing the twist pitch of the filaments in the wire. To achieve a 25% reduction in total hysteresis loss for fields cycled between 3 and –3 T, twist pitches as small as 2.5 mm are required. We define a characteristic length whose reciprocal is equal to the sum of the reciprocals of the sample length and the twist pitch. The result is a universal curve for hysteresis

loss as a function of characteristic length for different sample lengths and twist pitches.

II. PREPARATION OF SAMPLES WITH DIFFERENT TWIST PITCH

The Nb₃Sn conductor studied is described in Table I. It is the same as sample X in Ref. 14 and sample C in Ref. 15, and similar to sample 9 in Ref. 6. An unreacted wire segment was etched in 50% nitric acid to remove the exterior copper matrix. Striations on the Ta diffusion barrier were examined under a microscope to determine the as-supplied twist pitch, $\lambda_t = \pi D / \tan \phi$, where D is the diameter of the etched wire and ϕ is the angle made by the striations with respect to the wire axis. A continuous strand of wire was then prepared with six sections, each with a different λ_t .

The first section was untwisted clockwise using an electric drill until the filaments were about parallel to the wire axis. A longitudinal stripe initially painted on the wire aided in determining the number of twists removed. (The first several revolutions of the drill simply applied torsion to the wire but caused no plastic deformation.) The second section was left in the as-supplied condition, with $\lambda_t = 9.7$ mm. Subsequent sections had counterclockwise twist progressively added to the wire, thereby reducing λ_t to 2.5 mm in the sixth section of the strand. Filaments near the wire axis are only slightly transposed in twisted wire; filaments farther from the axis form larger helices.

The wire strand was then wound with right-hand turns on an oxidized stainless steel reaction mandrel, 4 mm in diameter. The wire axis was almost perpendicular to the mandrel axis and no twist was added or subtracted during winding. Small segments of each section were kept straight (along the side of the mandrel) for later measurement of critical current. The strand was reacted at 700 °C for 46 h in vacuum. We used “cold tails,” with the ends of the strand at room temperature to prevent tin leakage.

After reaction, the straight and coiled samples were cut with pliers. Optical microscopy of polished cross sec-

TABLE I. Characteristics of Nb₃Sn wire.

Wire identification	IGC 5901-8
Year manufactured	1985
Billet design	Double stack
Number of bundles	37
Number of filaments per bundle	150
Total number of filaments	5550
Wire diameter	
Before twisting, $\lambda_t=9.7$ mm	0.68 mm
After twisting, $\lambda_t=2.5$ mm	0.70 mm
Filament diameter (approximate)	
Nb, before reaction	2.7 μ m
Nb ₃ Sn, after reaction	3.0 μ m
Filament separation (edge-to-edge, from micrographs)	
Nb, before reaction	0.6–1.2 μ m
Nb ₃ Sn, after reaction	0–0.8 μ m
Cu/Nb local area ratio	1.5
Cu/non-Cu area ratio	0.88
Wire composition (mass percent, as designed)	
Cu stabilizer	47.0%
Ta diffusion barrier	7.1%
Superconductor (Nb 24.5%, Sn 16.5%, Cu 59.0%)	45.9%
Residual Sn (mass percent, estimated)	6%
Critical current at 7 T (average, 10 μ V/m criterion) ^a	300 A

^aSee Refs. 14 and 15.

tions showed a fair amount of filament contact in the filament bundles. There was no detectable difference in filament diameter from sample to sample; the slight reduction of the outer filaments expected as a consequence of twisting may be compensated by a small increase in wire diameter and decrease in wire length. Comparison photomicrographs suggest that one of the causes of filament contact for this wire and reaction schedule is the gathering of filaments around the periphery of each filament bundle during reaction, with an increase in area of the Cu-Sn core of each bundle. That is, the inner filaments in each bundle migrate toward the outer filaments. Another cause is the usual increase in filament diameter during reaction.

As a check on filament breakage, measurements on the straight segments in perpendicular field showed that twisting prior to reaction had no effect on the transport critical current of the six sections, within experimental accuracy. In fact, no difference is expected: Even though samples with small λ_t have parts of the outermost filaments oriented about 60° to the field, the critical current is limited by the parts oriented 90° to the field.¹⁶

III. MAGNETIZATION MEASUREMENTS AND CHARACTERISTIC LENGTH

Magnetization was measured in liquid helium at 4.2 K with a vibrating-sample magnetometer with the field along the axis of the sample coils, approximately transverse to the wire axis. Each sample coil was 5.4 mm in outer diameter and about 7 mm in height. The magnetometer was calibrated with similar coil of Ni wire. The field was swept between ± 3 T, well above the full-penetration field of the filaments, and data were acquired as the field changed. Some measurements were made up to 7 T. By comparing

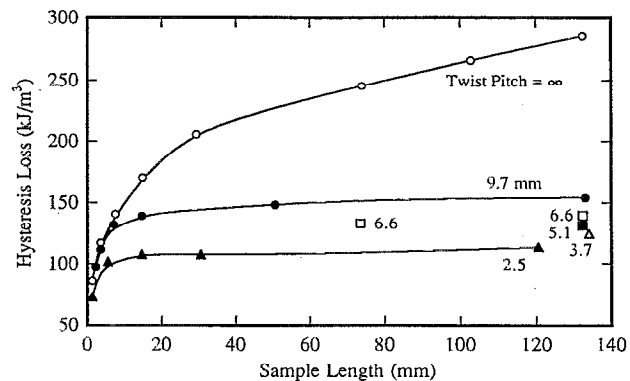


FIG. 1. Magnetic hysteresis loss W as a function of sample length l_s for coil samples with different twist pitch λ_t . W is very dependent on l_s for $l_s < \lambda_t$.

several sweep rates, we found that a rate of 0.375 T/min was slow enough to allow eddy currents to completely decay in all samples. Thus, the losses reported here are time-independent hysteresis losses, with no eddy-current contributions.

Figure 1 is a plot of hysteresis loss per total wire volume W for samples of different twist pitch λ_t and sample length l_s . Coil turns, or fractions of a turn, were removed, one at a time, to reduce a sample coil's height and l_s . As a function of l_s , W increases to saturation, with a knee at $l_s \approx \lambda_t$. Thus, to obtain a value of W that is representative of values obtained by other methods such as liquid-helium-boiloff calorimetry on large coils, l_s should be several times λ_t . The curve for the sample with nominally infinite λ_t does not saturate for the range of l_s studied. This is a master curve in the sense that curves for samples with decreasing values of λ_t branch off from it at progressively smaller values of l_s . The saturating dependence of loss on l_s is reminiscent of the length dependence of loss due to eddy-current coupling.⁸ The intrinsic loss of ideally isolated filaments would correspond to the axis intercept of the curves, at $l_s=0$.

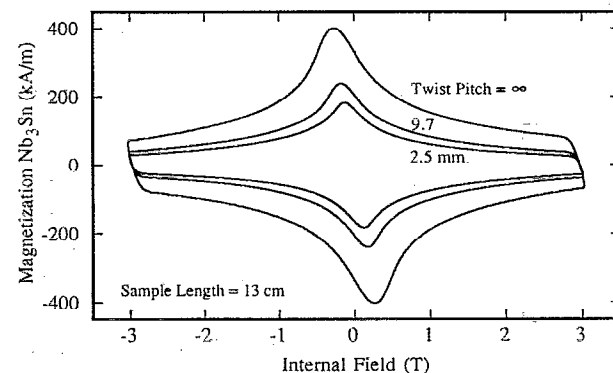


FIG. 2. Hysteresis loops of Nb₃Sn magnetization as a function of internal field for samples with $l_s \approx 13$ cm. The magnetization peaks in the second and fourth quadrants are those expected from the critical state of the filaments and a field-dependent critical current density. The curves are composed of individual data points.

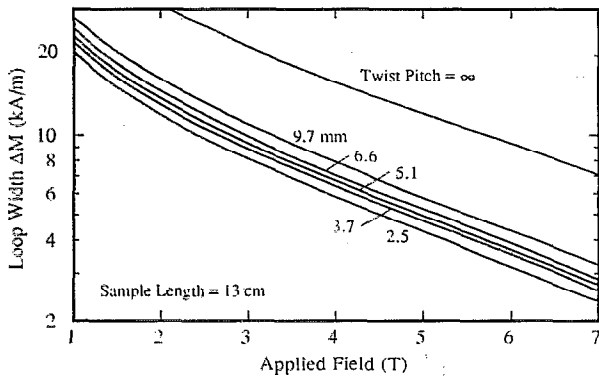


FIG. 3. Width of hysteresis loops as a function of positive applied fields for sample coils with $l_s \approx 13$ cm and different λ_t . Magnetization is reduced by decreasing λ_t , even for fields up to 7 T.

Figure 2 shows hysteresis loops for three of the samples with different λ_t and approximately constant l_s in which Nb_3Sn magnetization (magnetic moment per unit volume of Nb_3Sn) is plotted as a function of internal field H_i . Here, H_i is calculated from the applied field H_a as $H_i = H_a - NM$ using a demagnetizing factor N of 0.5. (This equation is rigorously correct only for uniformly magnetized infinite cylinders in transverse field; superconductors in the mixed state do not have uniform magnetization.) The volume fraction of Nb_3Sn in the reacted wire was assumed to be about 15% based on the data in Table I. The peaks in the second and fourth quadrants (near the magnetization axis) arise from the critical state of the filaments and a field-dependent critical current density. There is no apparent proximity coupling. Proximity coupling would give sharp peaks centered at zero internal field because positive and negative interfilamentary fields are equally effective in destroying the coupling.

The width of the hysteresis loops ΔM per total wire volume as a function of positive applied fields is plotted in Fig. 3 for different λ_t . The excess magnetization for increasing λ_t is not confined to low fields; rather, it occurs at all fields. Thus, the excess loss is not due to proximity effect. The effective filament diameter d_{eff} for the sample with the shortest λ_t is $7 \mu\text{m}$, based on the critical-state equation for cylinders in transverse field⁴ $d_{\text{eff}} = 3\pi\Delta M / (4J_c)$, where ΔM and J_c , the critical current density per total wire area, are taken at 7 T. This is large compared to the actual filament diameter $3 \mu\text{m}$, which indicates that joined filaments remain coupled up to at least 7 T. Figure 4 is a plot of W , for field cycles of ± 3 T, as a function of the reciprocal of a characteristic length L_c , where $L_c^{-1} \equiv l_s^{-1} + \lambda_t^{-1}$. In terms of W , samples with large l_s and small λ_t are equivalent to samples with small l_s and large λ_t , and the points seem to follow a simple logarithmic curve.

With decreasing L_c , d_{eff} would approach the mean filament diameter $3 \mu\text{m}$ if interfilament contact were only intermittent. In fact, even for L_c as small as 2 mm, d_{eff} is still about $7 \mu\text{m}$; this indicates that many filaments are in continuous contact. To verify this, we sanded and polished

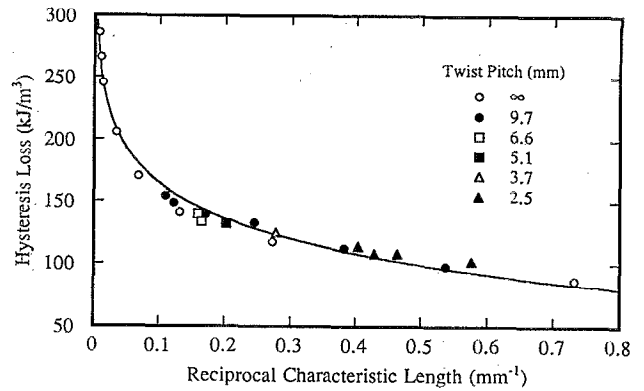


FIG. 4. Dependence of hysteresis loss W on reciprocal characteristic length $L_c^{-1} \equiv l_s^{-1} + \lambda_t^{-1}$. In terms of W , samples with large l_s and small λ_t are equivalent to samples with small l_s and large λ_t .

a straight, untwisted, reacted, etched, 10 mm sample longitudinally, through the Ta barrier. After the bronze matrix was etched, we examined the filaments under a microscope. Roughly 70% of the filaments were isolated, 20% were bonded in pairs, and 10% were in groups of three or more. The filaments that were in contact were joined over most of the sample length.

The mechanism for contact loss is directly analogous to that of interfilament eddy-current coupling loss. The filament twist causes a reduction of the areas of the shielding-current loops in transverse field. The difference is that contact loss is persistent whereas eddy-current loss is transient. For contact loss, the current paths are confined to the filaments and do not include the matrix. Unlike proximity-coupling loss, contact loss is maintained at high fields. Proximity coupling is absent because of the high resistivity of the Cu-Sn matrix. The small twist pitches required to achieve a significant reduction in hysteresis loss might be difficult to implement in practice. It would be preferable to avoid the problem by minimizing interfilament contact in the production of Nb_3Sn wires, perhaps by increasing filament separation and adjusting the reaction schedule to prevent migration of the filaments.

IV. EXPERIMENTAL PARAMETERS

We compared several experimental parameters for the magnetic determination of hysteresis loss using another Nb_3Sn wire ($\lambda_t = 14$ mm) from the same manufacturer. We think the results are applicable to all commercial internal-tin Nb_3Sn wires. We found that there was no difference among data obtained using a vibrating-sample magnetometer, a superconducting-quantum-interference-device (SQUID) magnetometer, and an extraction magnetometer, provided that each instrument was calibrated. In particular, SQUID magnetometers should be calibrated with standards of geometry similar to the samples. This especially applies to samples that produce nondipolar fields, such as long samples or those whose mass is distributed about their circumference. Use of the dipole calibra-

tion provided in the magnetometer software underestimates magnetization values by up to 10% for coil samples.

For this wire, hysteresis loss was a saturating function of I_s , similar to the curve for $\lambda_L=9.7$ mm in Fig. 1. We found no difference in hysteresis loss between coil samples cut with a diamond saw and polished and samples cut with pliers. (However, some end proximity effects at low fields may be noticeable in very small samples.) There was no dependence on bending radius from infinity (straight segment) down to at least 2 mm. There was no short-range inhomogeneity in the wire that might affect the magnetization measurements. Unlike the effect on transport critical current, severe mechanical strain of a coil sample after reaction had almost no effect on the magnetization. Thus, magnetization measurement discrepancies occasionally reported in interlaboratory comparisons on Nb₃Sn made by the internal-tin-diffusion process may be attributed mostly to differences in I_s .

ACKNOWLEDGMENTS

The wire was manufactured by Intermagnetics General Corporation (now IGC Advanced Superconductors Inc.) and supplied by M. Suenaga (Brookhaven National Laboratory). We had valuable discussions with F. R. Fickett (National Institute of Standards and Technology) and J. C. McKinnell (Teledyne Wah Chang Albany), and helpful comments on the manuscript from H. Wada (National

Research Institute for Metals) and J. W. Ekin (National Institute of Standards and Technology). This work was supported by the Science and Technology Agency of Japan; the Office of Fusion Energy, U.S. Department of Energy; and the Plasma Fusion Center, Massachusetts Institute of Technology.

- ¹S. S. Shen, "Magnetic properties of multifilamentary Nb₃Sn composites," in *Filamentary A15 Superconductors*, edited by M. Suenaga and A. F. Clark (Plenum, New York, 1980), pp. 309-320.
- ²S. S. Shen and J. D. Verhoeven, *IEEE Trans. Magn.* **17**, 248 (1981).
- ³A. I. Braginski and J. Bevk, "Alternating current losses in twisted *in-situ* composite wires," in *Filamentary A15 Superconductors*, edited by M. Suenaga and A. F. Clark (Plenum, New York, 1980), pp. 321-330.
- ⁴A. I. Braginski and G. R. Wagner, *IEEE Trans. Magn.* **17**, 243 (1981).
- ⁵A. K. Ghosh, K. E. Robins, and W. B. Sampson, *IEEE Trans. Magn.* **21**, 328 (1985).
- ⁶R. B. Goldfarb and J. W. Ekin, *Cryogenics* **26**, 478 (1986).
- ⁷A. K. Ghosh and M. Suenaga, *IEEE Trans. Magn.* **27**, 2407 (1991).
- ⁸M. N. Wilson, G. R. Walters, J. D. Lewin, and P. F. Smith, *J. Phys. D: Appl. Phys.* **3**, 1517 (1970).
- ⁹G. H. Morgan, *J. Appl. Phys.* **41**, 3673 (1970).
- ¹⁰W. J. Carr, Jr., *Adv. Cryo. Eng. (Materials)* **28**, 581 (1982).
- ¹¹N. Harada, Y. Mawatari, O. Miura, Y. Tanaka, and K. Yamafuji, *Cryogenics* **31**, 183 (1991).
- ¹²W. J. Carr, Jr., *J. Appl. Phys.* **54**, 6549 (1983).
- ¹³M. D. Sumption and E. W. Collings, *Adv. Cryo. Eng. (Materials)* **38**, 783 (1992).
- ¹⁴L. F. Goodrich and S. L. Bray, *Cryogenics* **29**, 699 (1989).
- ¹⁵K. Tachikawa, K. Itoh, H. Wada, D. Gould, H. Jones, C. R. Walters, L. F. Goodrich, J. W. Ekin, and S. L. Bray, *IEEE Trans. Magn.* **25**, 2368 (1989).
- ¹⁶L. F. Goodrich and F. R. Fickett, *Cryogenics* **22**, 225 (1982).